CONF-751101--75

HEDL-SA-974

CORRELATION OF CREEP AND SWELLING WITH FUEL PIN PERFORMANCE

R. J. Jackson, D. F. Washburn, F. A. Garner, and E. R. Gilbert

September 1975

Paper to be presented (1) at American Nuclear Society 1975 Winter Meeting, San Francisco, CA, November 16-21, 1975, and (2) at US-German Information Exchange at ERDA-RRD Headquarters, Washington, DC, during week of October 13, 1975.

This paper is based on work performed by Hanford Engineering Development Laboratory, Richland, Washington, operated by Westinghouse Hanford Company, a subsidiary of Westinghouse Electric Corporation, under United States Energy Research and Development Administration Contract E(45-1)-2170.

CORRELATION OF CREEP AND SWELLING WITH FUEL PIN PERFORMANCE

R. J. Jackson, D. F. Washburn, F. A. Garner, and E. R. Gilbert

The HEDL PNL-11 experiment was one in a series of fueled subassemblies irradiated in EBR-II to demonstrate the adequacy of the FFTF fuel pin design. The design variables are shown in Table 1. The cladding material, dimensions, and fuel density are prototypic of FFTF. Because neutron flux in EBR-II is lower than in FFTF, the uranium enrichment is higher in these experimental fuel pins, irradiated in EBR-II, than the FFTF enrichment for comparable linear heat rates. Table 2 lists some pertinent operating conditions for the center fuel pin in this experiment. This 37-pin subassembly represents, at 110,000 MWd/MTM, the highest burnup yet attained by a prototypic FFTF subassembly. Similarly, this is the highest fluence presently attained by prototypic fuel pins. A cladding breach occurred in one fuel pin which is presently being examined.

Figure 1 shows the measured dimameter increase along the length of the fuel column for the fuel pin PNL-11-9R. The profilometry was obtained from a spiral trace before removing the spacer wire. The axial profilometry, which was obtained after removing the wire, is the average of four traces 45° apart. These two sets of measurements agree within the measurement accuracy. The maximum diameter increase of 1.6 to 1.7% occurs 8 to 10 inches (20 to 25 cm) above the bottom of the core. This corresponds to 1-1/2 to 3-1/4 inches (4 to 8 cm) above the core midplane. The spiral trace indicates a secondary peak at about 3 inches (8 cm), whereas the axial trace has only an inflection point at that location.

The 37 PNL-11 fuel pins which finished their irradiation with EBR-II Run 50H have calculated burnups within the range 108,250 to 111,850 MWd/MTM calculated pin powers within 0.03 kW/ft (1 w/cm), calculated peak cladding inner surface temperature at the top of the fuel column within 11°F (6°C) of each other, and peak diameter increases in the range 1.3 to 2.1%. The location of the peak diameter increase was generally 8 to 10 inches (20 to 25 cm) above the bottom of the fuel column with a few fuel pins having measured diameter increases slightly out of this range. The peak cladding inner surface temperature at the top of the fuel column was calculated to be between 944 and 971°F (506 and 522°C) for those pins on the edge and between 1012 and 1040°F (544 and 560°C)

for the interior pins in the bundle. The interior fuel pin PNL-11-9R had a measured diameter increase of 1.7%, which was in the middle of the range. This was the basis for selecting this fuel pin for subsequent destructive examination. The fuel pins PNL-11-10R and PNL-11-41 had almost the same calculated cladding temperature as PNL-11-9R. However, pins PNL-11-10R and PNL-11-41 had maximum diameter increases of about 2.1% and 1.3%, respectively, as compared with PNL-11-9R at 1.7%. Figure 2 compares the spiral trace measurements of the 9R and 10R fuel pins. As can be noted, the diameter increase in these two pins is almost the same except at the location of the maximum diameter increase. PNL-11-10R shows a secondary peak at about 4 inches (10 cm). Figure 3 compares the measured diameter increase in fuel pins PNL-11-9R and PNL-11-41. In these two fuel pins, the shape of the profilometry curves is similar, with pin 41 having less measured diameter increase. The secondary peak for fuel pin PNL-11-41 is shown at about 2 inches (5 cm) above the bottom of the fuel column.

Figure 4 compares the measured density changes with calculated values of swelling. The measurements are from 1/2 inch (1 cm) long specimens, thus the horizontal error bars represent 1/2 inch. The vertical error bars are drawn to represent ±0.1% uncertainty. This value is based upon our judgment of data scatter, although the measurement repeatability is within much less than 0.1%. The measured profile has its maximum value between 8 and 9 inches (20 and 23 cm) above the bottom of the core, with a secondary peak about 2 inches (5 cm) above the core bottom.

The calculated swelling is the sum of stress-free swelling, stress-assisted swelling, and precipitate densification. These were calculated by equations (1), (2), and (3), respectively, and are compared with each other and the measured swelling in Figure 5.

$$\Delta D_1/D_o = \frac{1}{300} R \left\{\phi t + \frac{1.0}{\alpha} \ln \left[\frac{1.0 + \exp(\alpha[\tau - \phi t])}{1.0 + \exp(\alpha\tau)}\right]\right. \quad (1)$$

where

$$R = \exp(-88.5499 + 0.531072T - 0.00124156T^2 + 1.37215 \times 10^{-6}T^3 - 6.140 \times 10^{-10}T^4)$$

$$\tau = 256.262 - 2.39381T + 0.00816677T^2 - 1.18508 \times 10^{-5}T^3 + 6.21367 \times 10^{-9}T^4$$

$$\alpha = 1.12 + 0.00689T$$

ϕt = (neutron fluence)/10^{22}, n/cm^2 (E >0.1 MeV)

T = cladding temperature, °C

$\Delta D_1/D_o$ = fractional change in cladding diameter due to stress-free swelling, in/in.

$$\Delta D_2/D_o = \frac{(\Delta D_1/D_o \; P \; \sigma_H)}{2} \qquad (2)$$

where $P = 7.5 \times 10^{-5}$, in^2/pound

σ_H = hoop stress, pound/in^2

$\Delta D_2/D_o$ = fractional change in cladding diameter due to stress-enhanced swelling, in/in.

$$\Delta D_3/D_o = -\frac{1}{300}\left[0.03 + 0.14\left(\frac{T - 371.0}{183.0}\right)\right] \qquad (3)$$

where

T = cladding temperature, °C

$\Delta D_3/D_o$ = fractional change in cladding diameter due to precipitate densification, in/in.

We used cladding mid-wall temperature for the metal temperature and calculated the hoop stress from the "thin"-wall equation for use in these equations.

There is good general agreement between the measured and calculated swelling values along the entire fuel column length. From the peak location (9-inch) upward, this agreement is especially good. In the region from zero to four inches (0 to 10 cm) above the bottom of the fuel, the two curves have a somewhat different shape. Over this distance, the time averaged cladding inner surface temperature ranged from 800 to 900°F (427 to 482°C). This corresponds with the temperature range of 440 to 480°C (824 to 896°F) which Anselin associated with the low temperature swelling peak observed in the high burnup fuel pins irradiated by France in the Dounreay Fast Reactor.[1] Anselin describes a higher temperature peak which occurs over a temperature range of 560 to 605°C (1040 to 1121°F). A calculated time averaged cladding inner surface temperature of 1040°F (560°C)

occurs at 12.7 inches (32 cm) above the bottom of the fuel column. This is clearly above the peak swelling location. Thus, based upon the results of this single pin observation, there may be confirmation of Anselin's low temperature swelling peak. However, the PNL-11-9R fuel pin has its high temperature peak at a calculated time averaged cladding inner surface temperature of 520°C compared with the 560 to 605°C range of Anselin.

The inelastic strains were calculated as the sum of irradiation creep, swelling enhanced irradiation creep, and thermal creep. The thermal creep was calculated using the equation contained in the Nuclear Systems Materials Handbook for 20% cold worked Type 316 stainless steel. The irradiation creep equations are (4) and (5), respectively.

$$\Delta D_4/D_o = 0.8696 \times 10^{-8} \; A \; B \; \sigma_H \qquad (4)$$

where

$A = 2.3 \; \phi t + 2.0 \times 10^5 \exp [-16000/R(T + 273)]$

$B = \phi t - 1.7 \; \text{Tanh} \; (\phi t/1.7)$

ϕt = (neutron fluence)/10^{22}, n/cm^2 (E >0.1 MeV)

R = universal gas constant, cal/mole°K

T = cladding temperature, °C

σ_H = hoop stress, pounds/in^2

$\Delta D_4/D_o$ = fractional change in cladding diameter due to irradiation creep, in/in.

$$\Delta D_5/D_o = 0.652 \; D \; \sigma_H \; (3 \; \Delta D_1/D_o) \qquad (5)$$

where

$D = 1 \times 10^{-5}$, in^2/pound

σ_H = hoop stress, pounds/in^2

$\Delta D_5/D_o$ = fractional change in cladding diameter due to swelling enhanced irradiation creep, in/in.

The results of these two equations and their sum with thermal creep are shown on Figure 6. The sum is the total calculated inelastic strain. The "measured"

inelastic strain is determined by subtracting the measured $\Delta V/3V$ value from the associated diameter increase. The comparison of these two strains on Figure 6 shows the measured inelastic strains to be always somewhat larger than the calculated values. The reason for this difference is not presently known. Potential reasons include fuel-cladding mechanical interaction, uncertainties in the operating conditions, uncertainties in material properties, or anisotropy of stress-assisted swelling. Our models indicate that stresses and strains from fuel-cladding mechanical interaction should be insignificantly small. Postirradiation observations of the fuel are expected to support this. Burnup measurements are expected to confirm the calculated fuel pin powers. Fission gas measurements are expected to confirm the cladding stress due to the gas pressure. Observations of the cladding microstructure will be used at least qualitatively to confirm the cladding temperature. It has been noted that if one assumes a cladding temperature uncertainty of 210°F (117°C) at the top of the fuel column (with corresponding less uncertainty at lower cladding locations), good agreement is achieved between the calculated and measured inelastic strains. However, these uncertainties in cladding temperature appear unreasonably large. Finally, irradiation creep data at fluences up to 1×10^{23} n/cm^2 will be used when available to confirm the irradiation creep calculations.

Figure 7 is a comparison of the calculated and measured diameter increase for fuel pin PNL-11-9R. The calculated diameter increase is somewhat less than the measured diameter increase. This is largely because of low calculated creep values. By contrast, the calculated and measured values for diameter increase are in reasonable agreement for fuel pin PNL-11-41. This is shown on Figure 8. A similar comparison for fuel pin PNL-11-10R, shown on Figure 9, indicates that the calculated values are somewhat lower than the measured values of diameter increase.

These three fuel pins were irradiated as interior pins in the same subassembly with almost identical calculated cladding inner surface temperatures and calculated fuel pin powers but with apparently significantly different diameter increase. We expect to find the reason for these differences in diameter increase related to uncertainties in the thermal hydraulics or to extrapolation in fluence values beyond the irradiation creep data upon which the equations are based. However, it may be that this is normal data scatter.

It is concluded that:

1. The calculated values of irradiation creep are less than the measured values for two of the three fuel pins analyzed;
2. Some data suggest a low temperature swelling peak in agreement with others; and
3. Good agreement was shown between calculated and measured values of cladding swelling in the PNL-11-9R fuel pin.

REFERENCE

1. F. Anselin, "Irradiation of DFR 409," BIST, October 1974, pp. 27-40.

TABLE 1

PNL-11 NOMINAL DESIGN VARIABLES

Cladding material	20% CW 316
Cladding OD, in (mm)	0.230 (5.8)
Cladding thickness, in (mm)	0.015 (0.38)
Fuel-cladding diametral gap, in (mm)	0.006 (0.15)
Fuel pellet density, g/cm^3	10.97
Fuel pellet density, % theoretical	89.7
^{235}U enrichment ($^{235}U/U$ total) %	65
Plutonium oxide fraction ($PuO_2/UO_2 + PuO_2$), %	25
Fuel oxygen to metal ratio	1.976

TABLE 2

PNL-11-9R IRRADIATION HISTORY

Fuel pin power, kW/ft/(w/cm)	11.9 (390) beginning of life
Peak cladding ID temperature, F/C	1027 (553) beginning of life
Midplane burnup, MWd/MTM	106,000
Midplane flux, $n/cm^2/sec$ (E >0.1 MeV)	2.45×10^{15}
Midplane fluence, n/cm^2 (E >0.1 MeV)	1.02×10^{23}

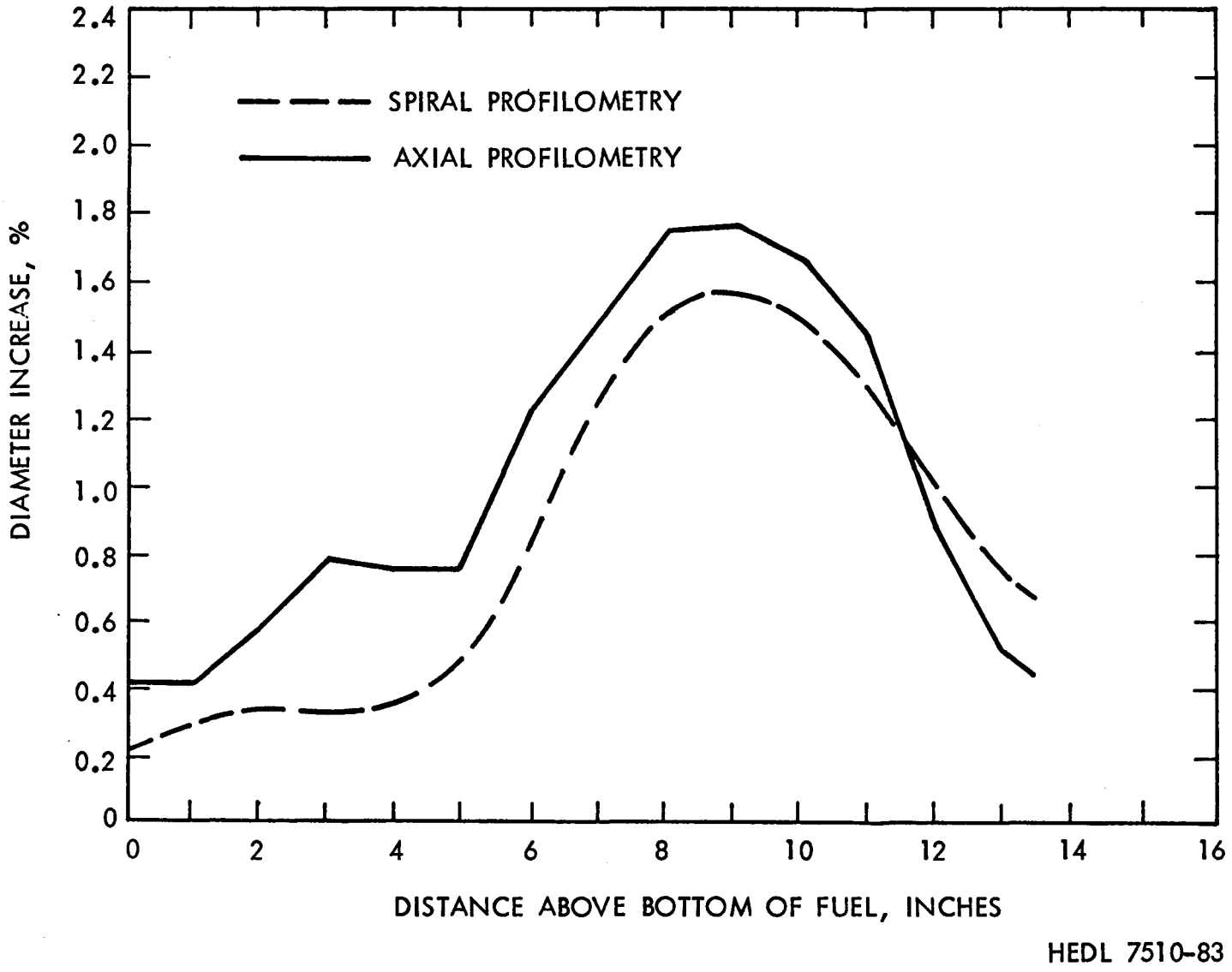

FIGURE 1. PNL 11-9R Measure Total ΔD/D.

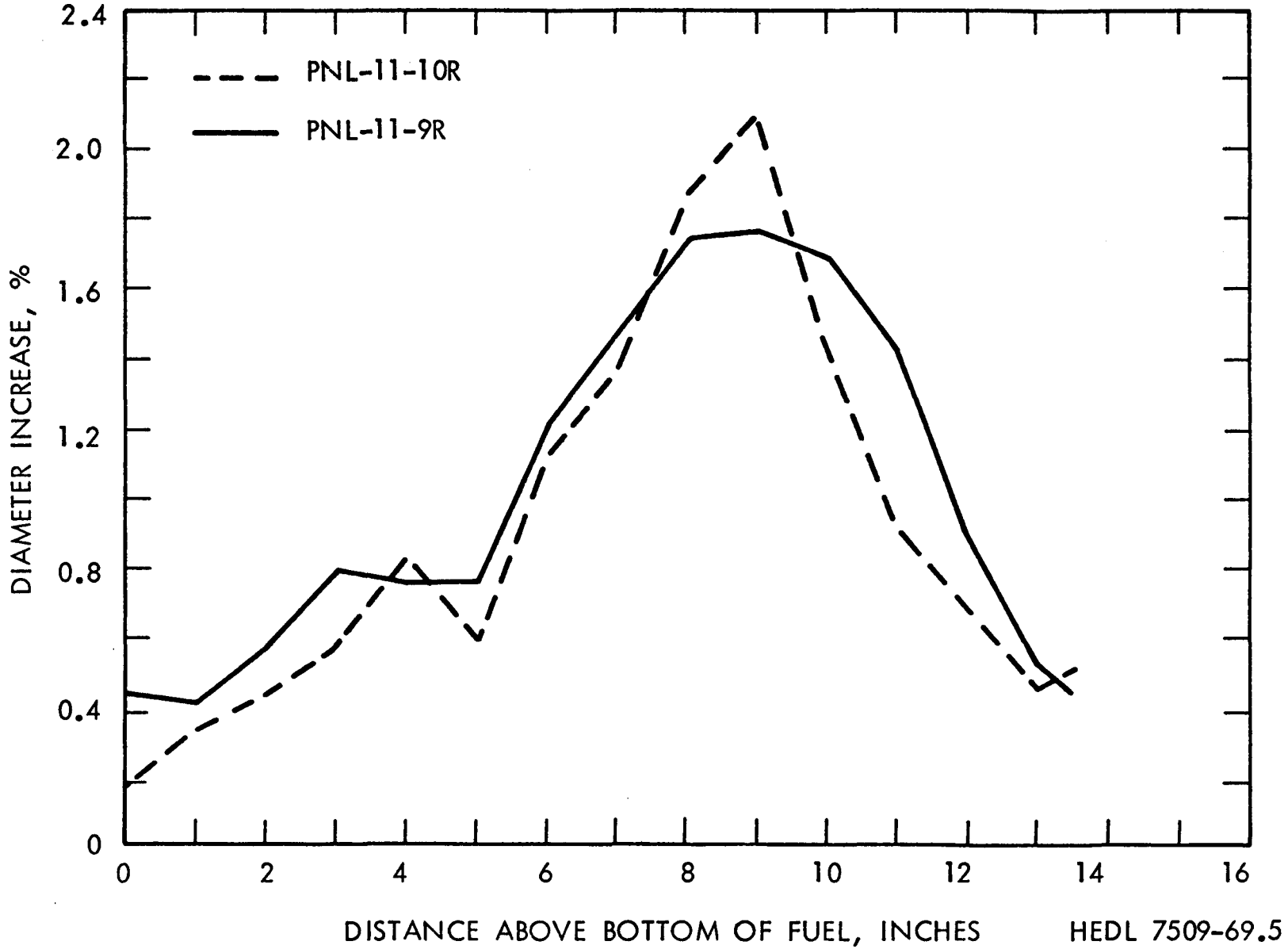

FIGURE 2. PNL 11-9R and PNL 11-10R Spiral Trace Measured Diameter Increase.

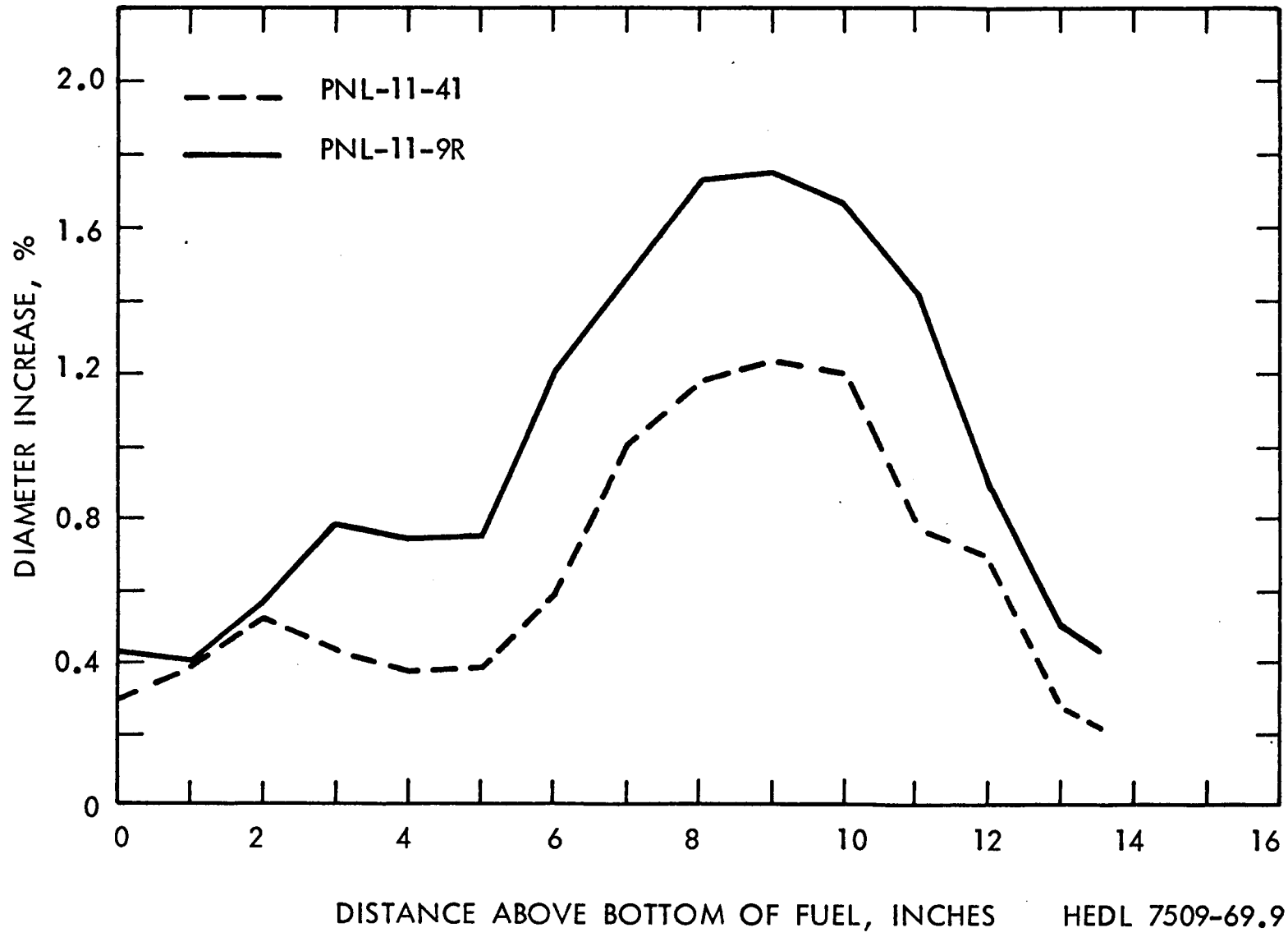

FIGURE 3. PNL 11-41 and PNL 11-9R Spiral Trace Measured Diameter Increase.

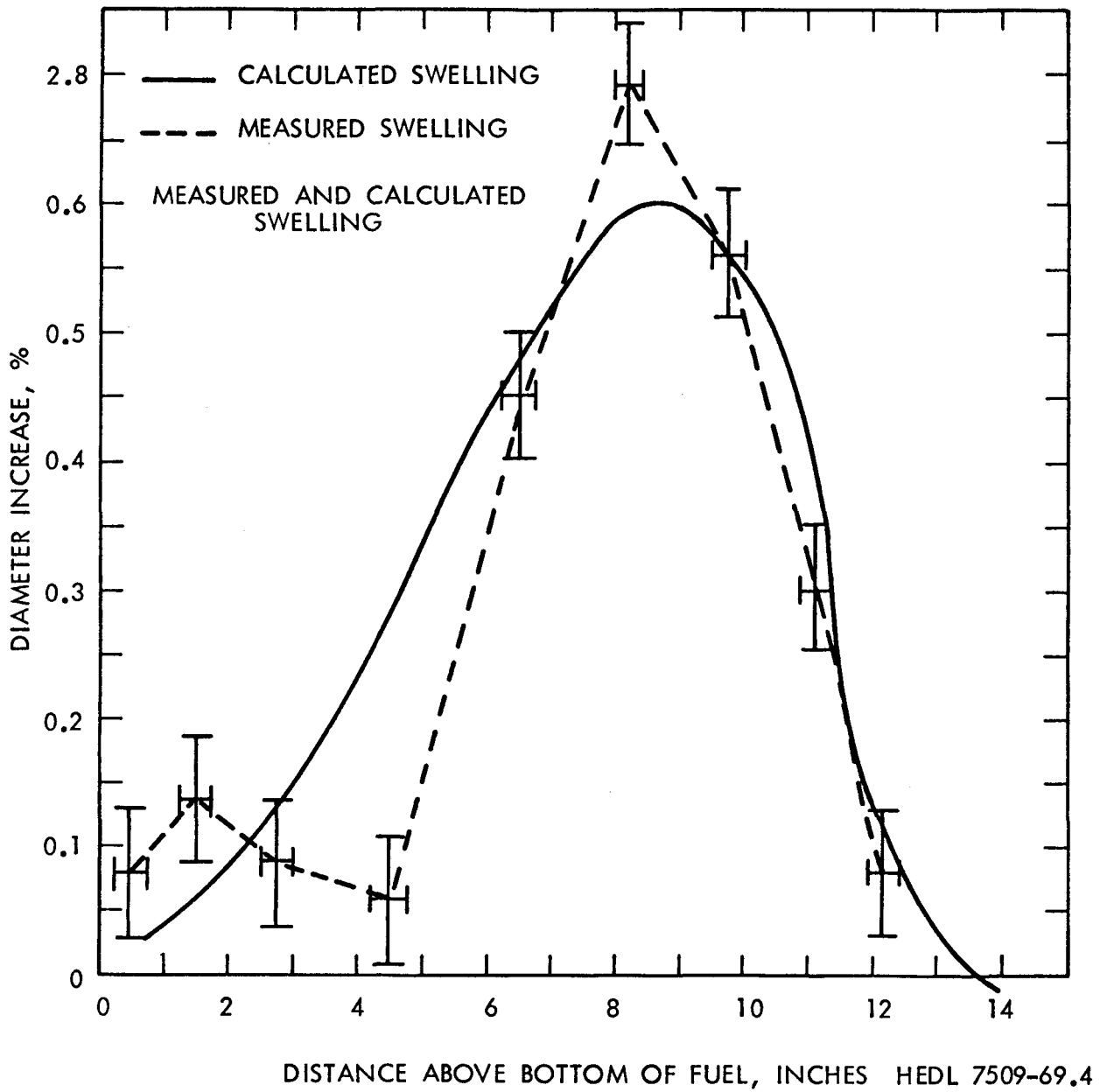

FIGURE 4. Swelling in PNL 11-9R.

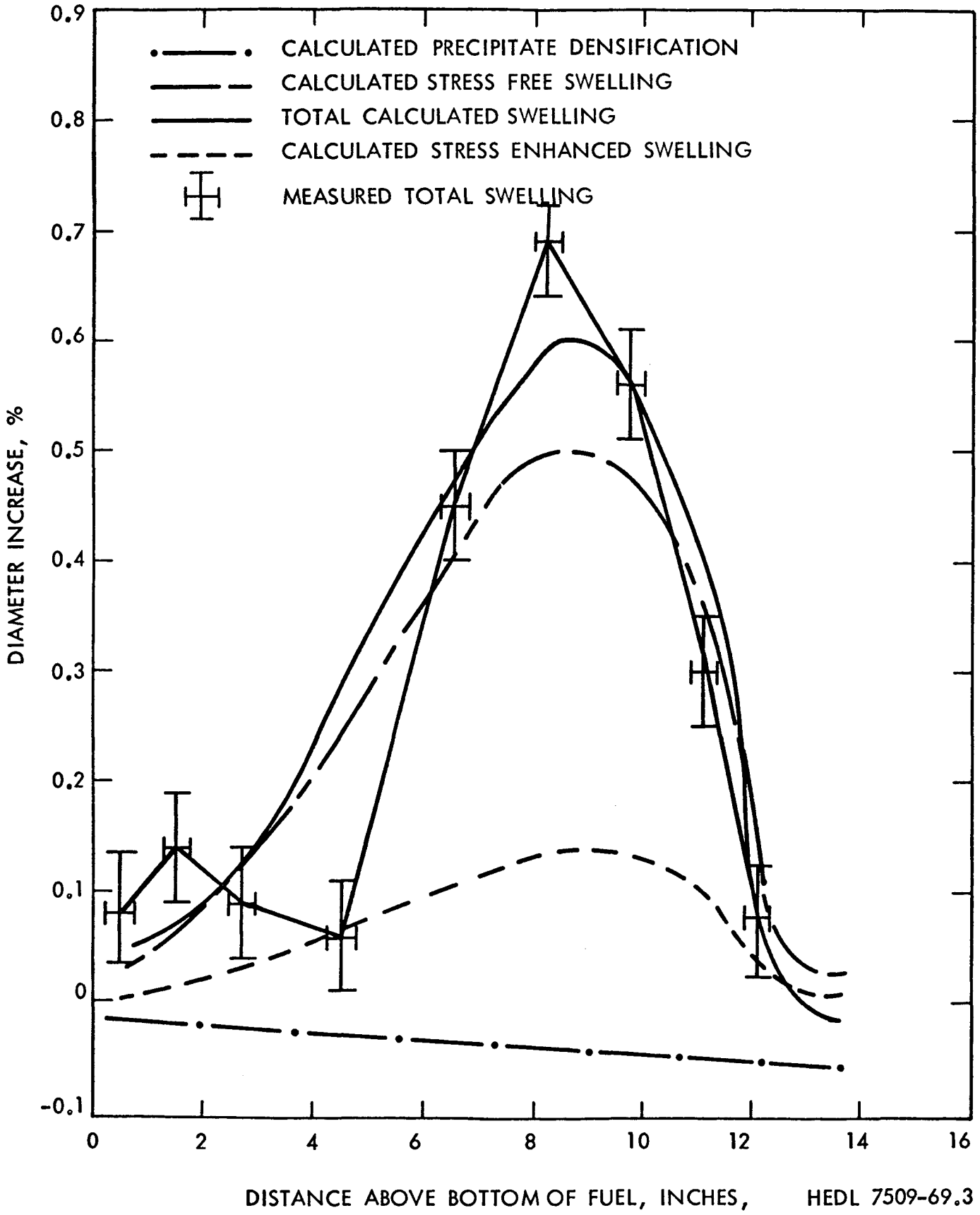

FIGURE 5. Swelling in PNL 11-9R.

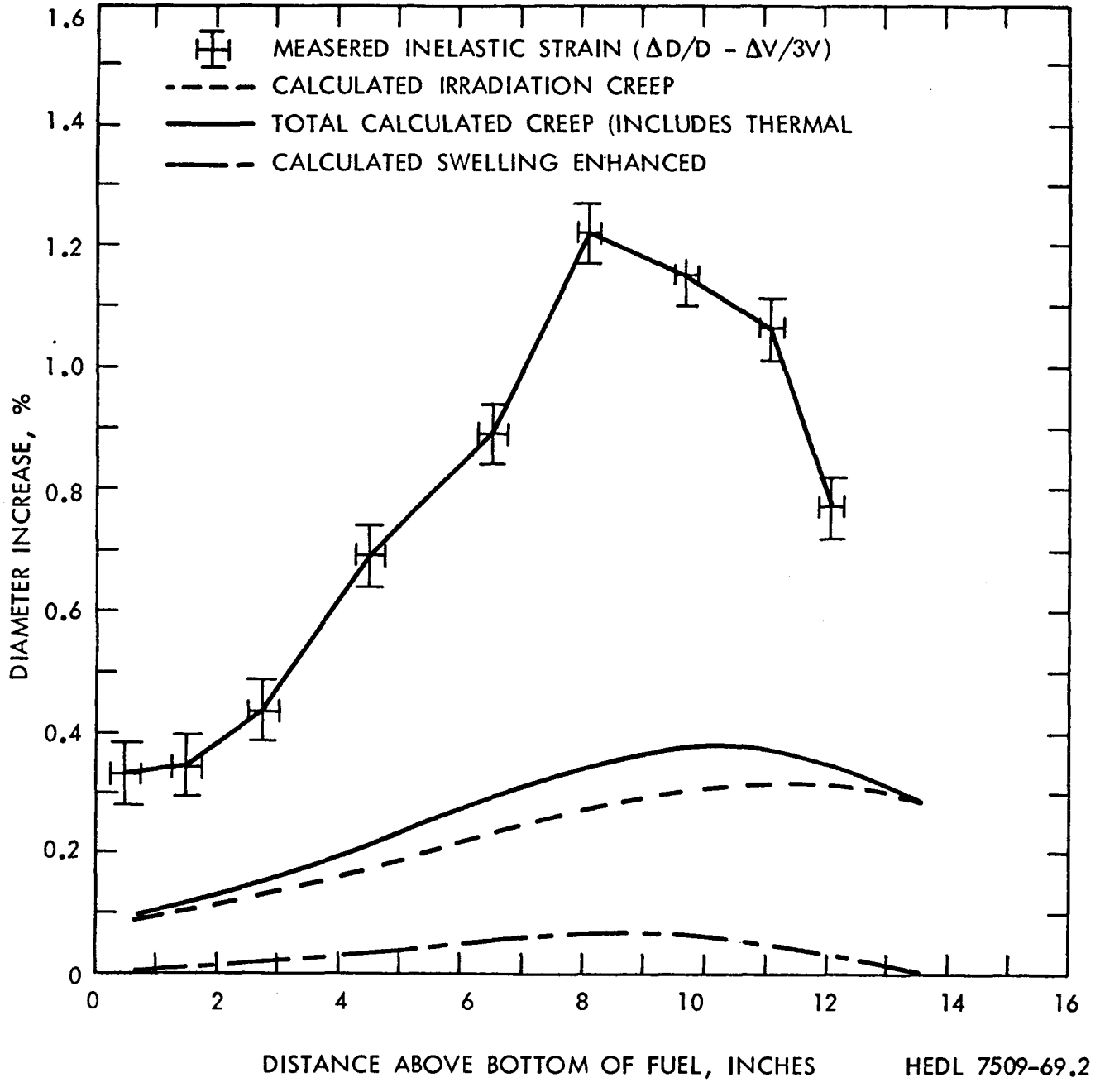

FIGURE 6. Inelastic Strain in PNL 11-9R.

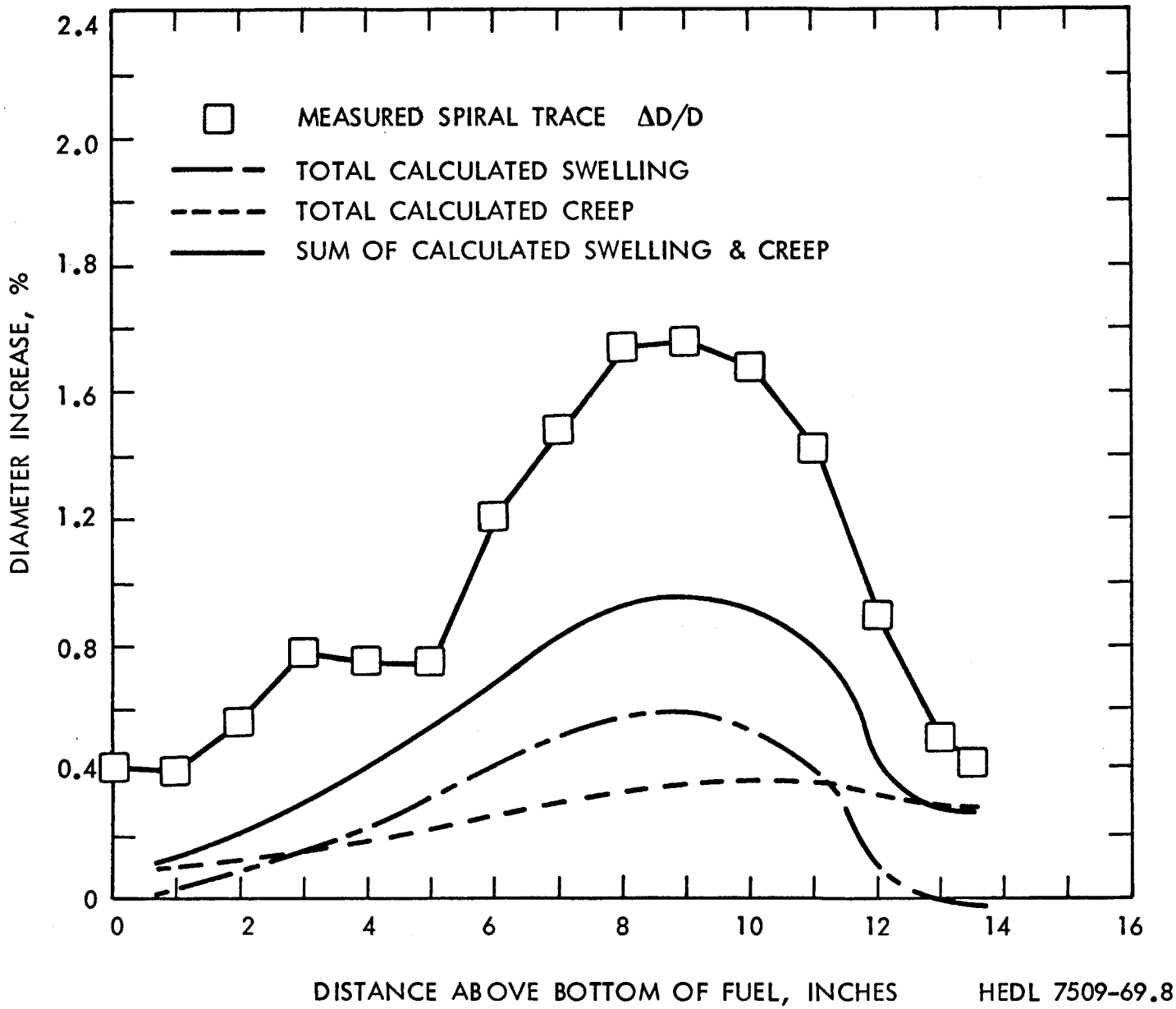

FIGURE 7. Diameter Increase for PNL 11-9R.

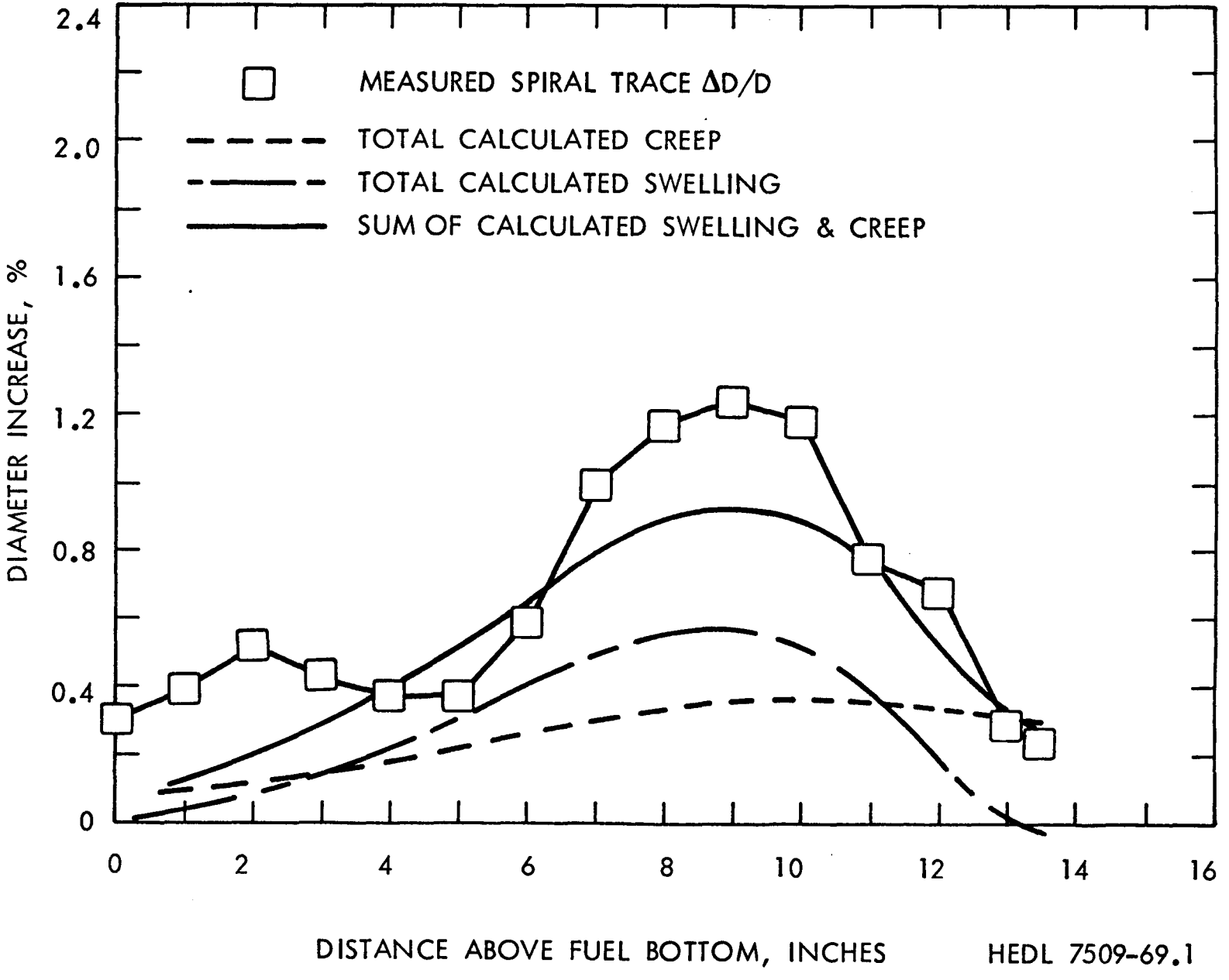

FIGURE 8. Diameter Increase for PNL 11-41.

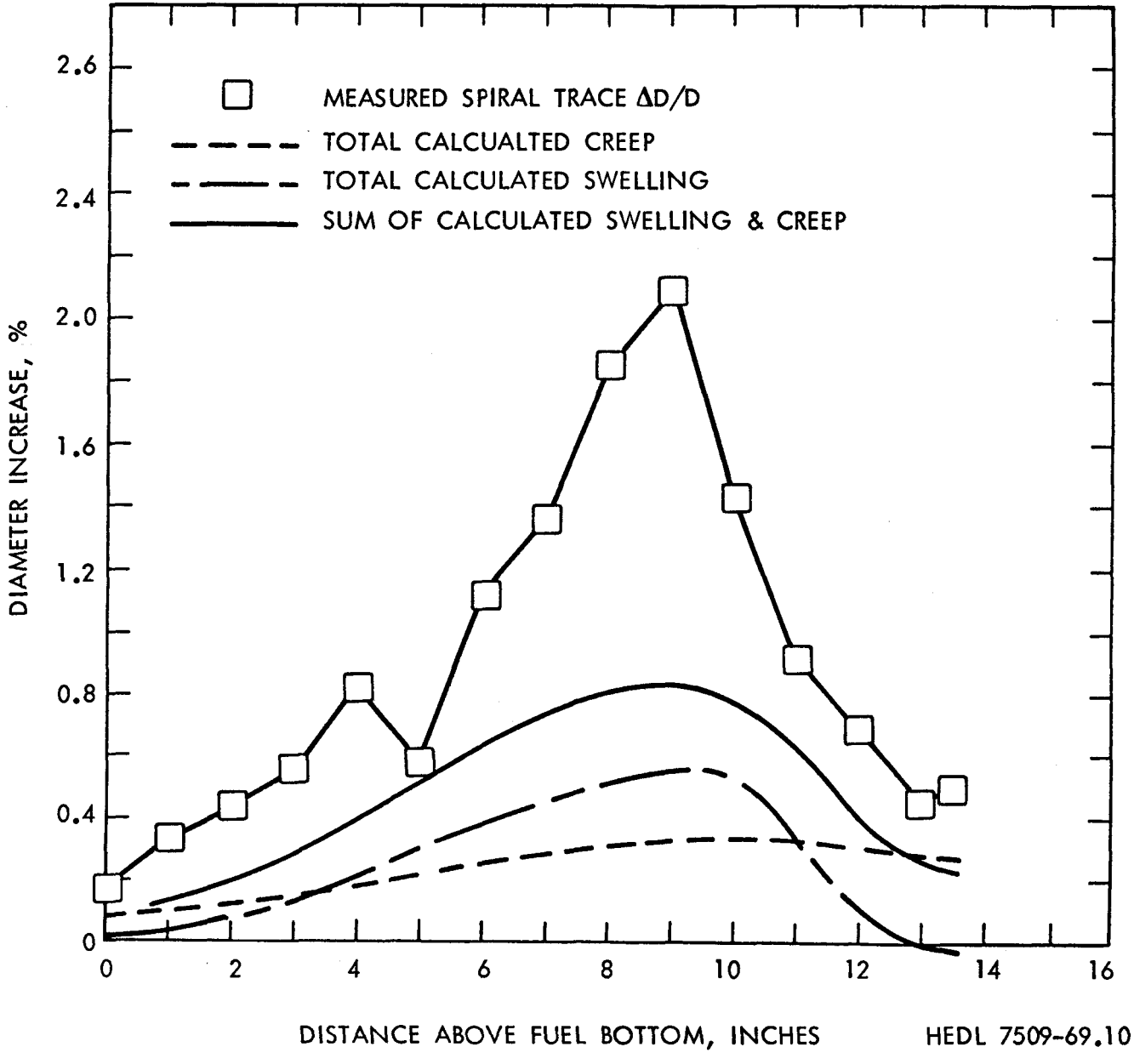

FIGURE 9. Diameter Increase for PNL 11-10R.